

**Loss of fungal symbionts at the arid limit of the distribution range in a native Patagonian grass – resource ecophysiological relations**

**Supporting information**

1.	APPENDIX s1. SUPPORTING METHODS .....	2
1.1.	Weather conditions derived from WorldClim database .....	2
1.2.	Soil particle size distribution and potential water availability .....	3
1.3.	Rhizosphere Soil.....	4
1.4.	Intrinsic water-use efficiency .....	4
1.5.	Oxygen isotope composition and stomatal conductance .....	5
1.6.	Data processing.....	6
1.7.	Statistical analyses .....	7
2.	APPENDIX s2. SUPPORTING TABLES.....	9
3.	APPENDIX s3. SUPPORTING FIGURES.....	18
4.	REFERENCES .....	27

## 1. APPENDIX S1. SUPPORTING METHODS

### 1.1. Weather conditions derived from WorldClim database

Apart from variables described in the main text, geographical coordinates were used to obtain minimum and maximum annual temperatures at a latitude/longitude resolution of 30 seconds from 50-year climatic means (1950-2000) of the WorldClim database ([www.worldclim.org](http://www.worldclim.org)) (Hijmans et al., 2005). The Pearson correlation between minimum and maximum annual temperature with mean annual temperature (MAT) were 0.8 and 0.9, respectively (Figure S7). Therefore, these two variables were not included in the statistical models.

Estimates of potential evapotranspiration (PET; mm year<sup>-1</sup>) were obtained from WorldClim minimum and maximum temperatures and latitude according to the function PET\_fromTemp in the EcoHydRology package in R (Fuka et al., 2014) that is based on the Priestley-Taylor (1972) equation. However, this variable was also not included in the model because it was highly correlated with mean and maximum annual temperature (Pearson correlation = 0.71 and 0.91, respectively).

The aridity index (AI), obtained as the mean annual precipitation (MAP) to potential evapotranspiration (PET) ratio, was used to evaluate the effect of precipitation surplus or deficit (UNEP, 1992). According to this index, aridity zones inside the survey area were defined as hyperarid if AI < 0.5, arid if 0.05 < AI < 0.20, semi-arid if 0.20 < AI < 0.50, dry subhumid if 0.50 < AI < 0.65 and humid if AI > 0.65. As AI and MAP were strongly correlated (Figure S7), those AI ranges were approx. equivalent to <65, 65-200, 200-500, 200-500 and >650 mm of MAP, respectively. The Pearson correlation between AI and MAP was 0.99 showing that precipitation was the dominant control on AI.

Atmospheric relative humidity (RH) was calculated as the ratio between actual vapor pressure ( $e_a$ , kPa) and saturation vapor pressure ( $e_{sat}$ , kPa), and expressed as a percentage ( $e_a/e_{sat} \times 100$ ). Saturation vapor pressure was estimated by using the minimum and maximum annual temperatures from the WorldClim database (1950-2000) according to Allen et al. (1998):  $0.6108 \times \exp((17.27 \times \text{temp}) / (\text{temp} + 237.3))$  where temp represents annual minimum or maximum temperature (in °C). The mean  $e_{sat}$  from minimum and maximum temperatures was taken as the effective saturation vapor pressure. Actual vapor pressure was obtained from the WorldClim v2.1 database (1970 – 2000). The Pearson correlation between mean annual precipitation (MAP) and atmospheric relative humidity (RH) was 0.84. Therefore, RH was not included in the statistical models.

Average maximum temperature from June to December 2014 – the growing season of *H. comosum* (Defossé et al., 1990) – was used in the estimation of intrinsic water use-efficiency (iWUE; see main text and below). Maximum temperature was estimated by the interpolation method. Climatic variables for the sampling-year growing season represented the conditions affecting growth of the

sampling-year shoot tissue that was collected for further analyses. We used monthly maximum temperatures available from 22 meteorological stations in the survey area (<https://www7.ncdc.noaa.gov/CDO/cdoselect.cmd>) to generate models (generalized linear model; glm function; R) which included elevation, longitude, latitude and average maximum temperature (long term climatic variable from WorldClim databased described above) as predictors. The meteorological stations included: El bolsón, Esquel aero, Maquinchao, San Carlos de Bariloche, Arroyo pescado, Corcovado, Cushamen, El hoyo, El maiten, Gobernador Costa, Gualjaina, l. Amutui quimei, Las golondrinas, Presa futaleufú, Puerto Bustillo, Río Futaleufú, Río Percy, Río Pico Vasquez, Río Senguer, Trevelin Incendios, Trevelin INTA, Valle del Corinto. We ran models for each month. Model assumptions on variance homogeneity and error normal distribution were graphically evaluated. We diagnosed multicollinearity by means of the vif function in car (Fox and Weisberg, 2011) and excluded terms with variance inflation factors (VIF) values above 1.5. Residual spatial correlation was evaluated by residual bubble in a coordinates plot as well as with semivariograms with and without four anisotropy factors. We did not find spatial correlation among residuals. Outlier removal of some stations was justified by the fact that there can be very local weather extremes which would have reduced the fit of the models. Finally, we predicted (predict function in R) monthly current maximum temperatures for the 30 sites of the survey. Values were averaged from June to December and expressed in °C. This approach of current weather conditions interpolation was also used to estimate mean and minimum temperature, precipitation and potential evapotranspiration (see Figure S7) and is similar to that described by Wittmer et al. (2008).

## **1.2. Soil particle size distribution and potential water availability**

Particle size was determined at site level by the pipette method described by Robison (1922) following Van Reeuwijk (2002) ([https://www.isric.org/sites/default/files/ISRIC\\_TechPap09.pdf](https://www.isric.org/sites/default/files/ISRIC_TechPap09.pdf)). The analysis comprised the fine earth <2 mm fraction. Cementing materials such as organic matter was removed by adding H<sub>2</sub>O<sub>2</sub> (30% in distilled water) to the sample placed in a beaker overnight. The next day, beakers were placed in a water bath held at 80 °C and 5 to 10 mL of H<sub>2</sub>O<sub>2</sub> was added several times until decomposition of organic matter was complete (i.e. the supernatant was clear). Then samples were dried, and 10 g of sample material used to determine the clay and silt fractions by the pipette method. After shaking with a dispersing agent (150 mL of 0.5% (v/v) sodium hexametaphosphate) for 90 minutes, the suspension was transferred to a 1 L polythene bottle. The bottle was filled with water to 1 L and placed in a water bath at room temperature to minimize fluctuations of temperature during the procedure. Temperature was recorded to calculate sedimentation time according to Stokes law. Depending on the temperature, sedimentation times were approximately 45 sec and 4 h for the <50 µm and <2 µm particle size fractions, respectively. Two

volumes of 20 mL were pipetted from the center of the cylinder at depths of 10 cm and 5 cm, respectively. The aliquots were transferred to tared moisture tins, evaporated on a water bath and dried overnight at 105 °C. The sand fraction was separated from the clay and silt fraction with a 52 µm sieve, dried overnight at 105 °C and weighed. Fractions of sand, silt and clay were expressed as percent of initial weight.

Potential soil water availability (PWA; % w/w) was estimated according to Saxton & Rawls (2006). This model estimated PWA based on soil particle distribution (i.e., clay and sand; % w/w), organic matter (estimated from total soil carbon content), pH and electrical conductivity (dS m<sup>-1</sup>; both 1:2.5 ratio soil to distilled water). The model includes a density factor which was set to 1 and gravel content which was set to zero. This variable allowed us to summarize the expected effect of several variables such as soil clay, organic matter, pH, and electrical conductivity on the response variables analyzed, thus permitting reduction of statistical model complexity. Pearson correlation between PWA and MAP was 0.67 (Figure S7) and MAP was preferred in the statistical models.

### 1.3. Rhizosphere Soil

Rhizosphere soil was collected from each plant. Soil chemical properties such as pH and electrical conductivity were measured in all rhizosphere soil samples (as mentioned above). Soil pH and electrical conductivity were determined on air-dried and sieved (2 mm) samples using a 1:2.5 soil/ distillate water ratio. Air dried soil samples were sieved to 2 mm, ground, and analyzed for total carbon (C) and nitrogen (N) concentration using an elemental analyzer (NA 1110; Carlo Erba Instruments). Pearson correlation between MAP and rhizosphere N was 0.71 (Figure S7). Therefore, rhizosphere N was excluded from the statistical models as predictor.

### 1.4. Intrinsic water-use efficiency

$\delta^{13}C_p$  (see main text) was used to calculate <sup>13</sup>C discrimination ( $\Delta^{13}C$ , see below) from which *iWUE*, the assimilation-weighted, growing season-integrated ratio of net photosynthesis (*A*) to stomatal conductance for water vapor (*g*<sub>H<sub>2</sub>O</sub>) was estimated according to Ma et al. (2021) as

$$iWUE = \frac{c_a}{k} \cdot \frac{b - \Delta - f \frac{\Gamma^*}{c_a}}{b - a_s + \frac{g_{sc}}{g_m} (b - a_m)} \quad (\text{Eqn 1})$$

In eqn 1, *c<sub>a</sub>* represents the atmospheric CO<sub>2</sub> concentration (in mole fractions), *k* (= 1.6) the ratio of the diffusivities of water vapor and CO<sub>2</sub>, *a<sub>s</sub>* the <sup>13</sup>C discrimination during diffusion of CO<sub>2</sub> in air through the stomatal pore (4.4‰), *a<sub>m</sub>* (1.8‰) the fractionation associated with CO<sub>2</sub> dissolution and diffusion in the mesophyll, *b* and *f* the fractionations due to carboxylation and photorespiration, *Γ\** the CO<sub>2</sub> compensation point in the absence of mitochondrial respiration calculated following Brooks and Farquhar (1985), and *g<sub>s</sub>/g<sub>m</sub>* the ratio of stomatal and mesophyll conductance. This model

improves predictions of iWUE by the simplified Farquhar model of  $^{13}\text{C}$  discrimination by also accounting for the effects of mesophyll conductance and photorespiration on  $^{13}\text{C}$  discrimination.

We estimated  $\Delta^{13}\text{C}$  as  $(\delta^{13}\text{C}_a - \delta^{13}\text{C}_p) / (1 + \delta^{13}\text{C}_p)$ , where  $\delta^{13}\text{C}_a$  ( $\delta^{13}\text{C}$  of atmospheric  $\text{CO}_2 = -8.37\text{‰}$ ) was obtained as the average from June to December 2014 (the growing season before sampling) measured at Ushuaia (the closest available monitoring site) according to the NOAA database ([https://gml.noaa.gov/aftp/data/trace\\_gases/co2c13/flask/surface/](https://gml.noaa.gov/aftp/data/trace_gases/co2c13/flask/surface/). Accessed Dec 2021).  $c_a$  was also estimated from the Ushuaia data from NOAA ([https://gml.noaa.gov/aftp/data/trace\\_gases/co2c13/flask/surface/](https://gml.noaa.gov/aftp/data/trace_gases/co2c13/flask/surface/). Accessed Dec 2021). We performed a linear regression between  $c_a$  and  $\delta^{13}\text{C}_a$  with the available data ( $R^2 = 0.96$ ) and used that regression to estimate  $c_a$  for the period June to Dec 2014, the growing season of sampled plants. Gamma star ( $\Gamma^*$ ) was estimated as  $\Gamma^* = 42.7 + 1.68 (T - 25) + 0.012 (T - 25)^2$ , with  $T$  the average maximum temperature in the period June to December 2014. The ratio of stomatal and mesophyll conductance was set constant and equal ( $= 0.79$ ) to that presented by Ma et al. (2021). According to Ma et al. (2021), that constant is similar for a wide range of plant functional groups and is unaffected by long-term drought conditions.

## 1.5. Oxygen isotope composition and stomatal conductance

The relationship between  $\delta^{18}\text{O}_p$  and stomatal conductance of plants growing in the same environment is connected with the fact that: 1) all oxygen in cellulose originates from water, 2) water becomes evaporatively  $^{18}\text{O}$ -enriched in leaves, causing an  $^{18}\text{O}$ -enrichment of primary photosynthetic products, 3) a certain fraction of the  $^{18}\text{O}$ -enrichment signal in photosynthetic products is retained during cellulose synthesis, and 4) leaf water  $^{18}\text{O}$ -enrichment is dependent on transpiration, which varies as a function of stomatal conductance, if atmospheric water demand is the same for all plants in the same environment (Barbour, 2007; Farquhar et al., 2007; Scheidegger et al., 2000).

The relationship between  $\delta^{18}\text{O}_p$  and stomatal conductance is uncertain when plants collected at different sites or at different times are compared. That complication is related to spatio-temporal variation of the  $\delta^{18}\text{O}$  of meteoric waters ( $\delta^{18}\text{O}_{\text{rain}}$ ) and climatic conditions (temperature, relative humidity, vapor pressure deficit) that affect  $\Delta^{18}\text{O}_p$  (Baca Cabrera et al., 2021; Cernusak et al., 2005; Hirl et al., 2021; Kahmen et al., 2011). To account for the effect of  $\delta^{18}\text{O}_{\text{rain}}$ , we calculated the  $^{18}\text{O}$ -enrichment of cellulose above  $\delta^{18}\text{O}_{\text{rain}}$  as  $\Delta^{18}\text{O}_p = (\delta^{18}\text{O}_p - \delta^{18}\text{O}_{\text{rain}})/(1 + \delta^{18}\text{O}_{\text{rain}})$ . Geographical coordinates were used to obtain the mean oxygen isotopic composition of local meteoric waters ( $\delta^{18}\text{O}_{\text{rain}}$ ) as estimated by the ECHAM5-wiso global simulation models (Werner, 2019). This data set contains monthly values of  $\delta^{18}\text{O}_{\text{rain}}$  from 15<sup>th</sup> January 1958 to 15<sup>th</sup> December 2013 with a resolution of longitude =  $1.125^\circ$  and latitude =  $1.121^\circ$ . Monthly data were averaged: 1) from June to December (1958-2013), the growing season of *H. comosum*; 2) from April to September (1958-2013), the rainy

season; and 3) April to September 2013, the rainy season previous to the sampling year. A clear seasonal pattern was not evident in those data.

$\Delta^{18}\text{O}_\text{P}$  was calculated using all three  $\delta^{18}\text{O}_\text{rain}$  alternatives and the corresponding statistical models gave all the same result. We used  $\Delta^{18}\text{O}_\text{P}$  calculated with  $\delta^{18}\text{O}_\text{rain}$  as the average of June-December from 1958 to 2013 (growing season) in the statistical models.

### Parameters

Model Parameters	1: Jun-Dec 1958-2013			2: Apr-Sept 1958-2013			3: Apr-Sept 2013		
	lower	est.	upper	lower	est.	upper	lower	est.	upper
(Intercept)	35.4	<b>37.5</b>	39.6	36.1	<b>38.2</b>	40.3	36.6	<b>38.8</b>	40.9
I(1/MAP)	40.1	<b>711.1</b>	1382.1	70.1	<b>739.1</b>	1408.1	120.2	<b>805.5</b>	1490.8
AMF	-0.1	<b>-0.04</b>	-0.01	-0.1	<b>-0.04</b>	-0.01	-0.1	<b>-0.04</b>	-0.01
P	-11.6	<b>-6.1</b>	-0.6	-11.6	<b>-6.1</b>	-0.6	-11.4	<b>-5.9</b>	-0.4
I(1/MAP) x AMF	0.9	<b>11.4</b>	22.0	1.0	<b>11.5</b>	22.0	1.1	<b>11.6</b>	22.2
<b>R<sup>2</sup></b>	0.78			0.79			0.8		
<b><math>\Delta</math> AICnull</b>	23.8			24.7			27		

## 1.6. Data processing

Considering that missing data can cause biased parameter estimations (Nakagawa & Freckleton, 2008, 2011), we used the multiple imputation statistical approach to handle problems related to randomly occurring missing data. We used the function `argImpute` in the `Hmisc` package in R (Harrell Jr and Dupont, 2016) which allowed grouping plant data by site according to the sampling design. We generated imputation for missing values of P concentration ( $n = 8$ ),  $\delta^{18}\text{O}_\text{P}$  ( $n = 5$ ) and *Epichloë* endophyte presence ( $n = 17$ ; in all cases, out of a total of 238). We set the procedure to five multiple imputations ( $n.\text{impute} = 5$ ) that gave the best statistical adjustment (i.e.,  $R^2$ ). These five values were then averaged to generate a single data set without missing values. Missing AMF colonization values were not included in this process. There were no missing values on site level variables.

The percentage of AMF colonization was determined according to McGonigle et al. (1990) and adjusted by subtracting observer bias prior to analyses. For that, we ran a null model (i.e., with no fixed effects) with observed as random and compared it with a null model without the random effect. The observed generated a bias as AIC was 64.6 lower in the first compared to the second case. We adjusted AMF colonization values by subtracting observer bias prior to analyses. One outlier value was replaced by the average of the corresponding site where *Epichloë* was not present.

## 1.7. Statistical analyses

We first modelled site-level traits to describe the influence of environmental variables (i.e., MAP and MAT) or grazing severity on vegetation cover and *H. comosum* cover. The vegetation cover model was a normal error distribution generalized least squares model (glS function in nlme package) and included MAP, MAT, grazing severity and the interaction between MAP and grazing severity as predictors. The *H. comosum* cover model was a generalized linear model with beta error distribution (betareg function with beta error distribution) and included MAP, MAT, grazing severity, vegetation cover and the interaction between MAP and grazing severity as predictors. In both models including transects as random effect or not gave a very similar likelihood (LRT: 2.4e-08; p-value = 0.99 and  $X^2 = 4e-04$ ; p-value = 0.98, respectively).

Then, we modelled plant-level traits to study the influence of environmental variables or grazing severity on *Epichloë* presence, AMF colonization, nitrogen and phosphorus concentration in shoot biomass,  $\Delta^{18}O_p$  and iWUE. *Epichloë* presence was analyzed with a generalized linear mixed model (GLMM) which accounted for individual plants nested in sites and sites nested in transects (Pinheiro & Bates, 2006) with binomial error distribution (Bates et al., 2015). This model included MAP, MAT, grazing severity and the interaction between MAP and grazing severity as main factors.

The other models at plant-level were analyzed by using linear mixed-effects models with the same nesting hierarchies (i.e., individual plants nested in sites and sites nested in transects) but with normal distribution of errors. Specifically, all models (AMF colonization, shoot nitrogen and phosphorus,  $\Delta^{18}O_p$  and iWUE) included MAT, MAP, grazing severity, *Epichloë* presence and the double interaction between the last three factor as fixed effects. Then, shoot nitrogen and phosphorus concentration,  $\Delta^{18}O_p$  and iWUE models also included AMF colonization and its double interactions with MAP, grazing severity and *Epichloë* presence.  $\Delta^{18}O_p$  and iWUE models included shoot nitrogen concentration and its double interactions with MAP, grazing severity and *Epichloë* presence. And the iWUE model included  $\Delta^{18}O_p$  and its double interactions with MAP, grazing severity and *Epichloë* presence as fixed effects (Table 1).

Before defining the initial model, we analyzed collinearity between given climatic and environmental variables with a Pearson correlation of 0.7 as threshold (Figure S7)(Dormann et al., 2013). The Pearson correlation between MAP and MAT was modest (-0.38) and did not show collinearity in the statistical model. Main predictors were centered by subtracting the mean value before fitting the models. This procedure largely removed the correlations and inflated standard errors for the main effects and improved the interpretation of estimated parameters (Schielzeth, 2010). Then we selected the most parsimonious random intercepts structure (transect/site or site) for the initial model by comparing the Akaike information criterion of the complete models estimated with

restricted maximum likelihood (REML) (Zuur et al., 2009). We evaluated multicollinearity on the initial and final models by means of the VIF (Table S2) (Dormann et al., 2013). We performed a graphical inspection of the models with normal error distribution to evaluate their adequacy (Pinheiro & Bates, 2006; Zuur et al., 2009). When necessary, the variances were modelled by using specific variance functions (Table S3). We did not find spatial correlation among residuals. In the case of the *Epichloë* presence model (binomial-Bernoulli model), the dispersion parameter indicated no overdispersion ( $\phi = 0.37$ ). The initial models estimated by ML were reduced by removing non-significant terms in a stepwise fashion (single term deletion strategy) according to likelihood ratio tests (Table 1 and Table S4-5) (Zuur et al., 2009). Multimodel inference performed with dredge function (MuMIn package in R; Barton, 2016) produced the same results. When *Epichloë*, grazing severity or an interaction involving them were significant, least squares means adjusted by “sidak” method and significant p-value  $< 0.05$  was used to compare means between levels of factors or slopes (emmeans and emtrends functions, respectively with emmeans package; Lenth, 2017) (Table S6). To validate the strength of fixed effects included in the minimum model, we calculated the difference between the AIC of the null and the minimum model (null model means the same model as the minimum model excluding all fixed effects;  $\Delta AIC$ ). We also present the conditional and marginal coefficient of determination ( $R^2_c$  and  $R^2_m$ , respectively from r.squaredGLMM function in MuMIn package; Barton, 2016). A summary with traits of the models is presented in Table S3.

Being aware of the effects of the atmospheric relative humidity (RH) and temperature on  $\Delta^{18}O_p$  (e.g., Hirl et al., 2021), we graphically evaluated the relationship of  $\Delta^{18}O_p$  with MAP for iso-atmospheric-relative humidity (iso-RH) and for isothermal gradients. The iso-atmospheric-relative humidity transect was defined as the range between the mean value of RH (58.6%)  $\pm 2\%$  which included 12 sites with  $\sim 300$  to 700 mm MAP (Figure S2). The isothermal transect was defined as  $8.4 \pm 0.25^\circ\text{C}$  and included 10 sites distributed along the entire MAP gradient (Figure S3). All analyses and figures were made in the R-cran environment; version 3.6.1 (R Development Core Team, 2019) and with RStudio; version 1.2.1335 (RStudio, 2019).

## 2. APPENDIX S2. SUPPORTING TABLES

**Table S1:** Criteria for the classification of sites in terms of the grazing conditions (mild and severe) according to vegetation cover and floristic composition. The first column shows the environments classified according to mean annual precipitation (MAP). Using a scenario of mild grazing as a reference condition, we established the expected abundance changes of both palatable and unpalatable forage species for each environment. The overall idea is that, with grazing intensity, valuable forage species tend to diminish while unpalatable species tend to increase (Based on Bonvissuto et al., 2008; Siffredi et al., 2011).

Environment	MAP	Vegetation cover (%)		Species present under mild grazing	
		Mild	Severe	Grasses	Schrub
Humid	>650	≥ 70	< 70	<i>Festuca pallescens, Poa ligularis,</i>	
Subhumid	650-500	≥ 60	< 60	<i>Hordeum comosum, Carex spp.</i>	
Semiarid	500-200	≥ 50	< 50	<i>Poa ligularis, Hordeum comosum,</i>	<i>Senecio filaginoides, Azorella</i>
Arid	<200	≥ 45	< 45	<i>Bromus setifolius, Pappostipa speciosa,</i>	<i>prolifera, Adesmia volcksmannii</i>

**Table S2:** VIF values of the initial and final regression models for *Hordeum comosum* analyses. Rows show the models for: vegetation cover, *H. comosum* cover, *Epichloë* presence, AMF colonization, nitrogen (N) and phosphorus (P) concentration in shoot biomass,  $\Delta^{18}\text{O}_\text{P}$  and iWUE. Columns show the VIF or GVIF (generalized VIF) depending on the model. In the cases where GVIF was calculated, we determined the threshold as  $10^{(1/(2*\text{df}_{\text{predictor}}))}$  where  $\text{df}_{\text{predictor}} = \text{vif}(\text{model})[,2]$ . VIF and GVIF were obtained with vif function in car package in R. When the final model had only one predictor (i.e., *H. comosum* cover, vegetation cover and *Epichloë* presence), VIF values made no sense.

	Initial model				Final model			
<i>H. comosum</i> cover (%)	GVIF	Df	GVIF <sup>(1/(2*Df))</sup>	Threshold	GVIF	Df	GVIF <sup>(1/(2*Df))</sup>	Threshold
poly(MAP, 2)	2.957833	2	1.311425	1.778279				
Grazing	34.006648	1	5.831522	3.162278				
MAT	2.137199	1	1.461916	3.162278				
Veg_cover	1.247686	1	1.116999	3.162278				
poly(MAP, 2): Grazing	67.184950	2	2.862978	1.778279				
Vegetation cover (%)	VIF				VIF			
MAP	2.344111							
Grazing	1.741470							
MAT	1.341390							
MAP:Grazing	2.203441							
<i>Epichloë</i> presence	VIF				VIF			
MAP	2.723662							
Grazing	1.804258							
MAT	1.315208							
MAP:Grazing	2.204771							
AMF colonization (%)	VIF				VIF			
MAP	11.503436				1.221396			
<i>Epichloë</i>	4.260555				1.221396			
Grazing	7.787651							
MAT	1.693648							
MAP: <i>Epichloë</i>	8.900665							
MAP:Grazing	2.769279							

**Table S2:** cont.

	Initial model				Final model				
	<i>Epichloë</i> : Grazing	9.221692							
Shoot N (%)		GVIF	Df	GVIF <sup>1/(2*Df)</sup>	Threshold	GVIF	Df	GVIF <sup>1/(2*Df)</sup>	Threshold
	<i>Epichloë</i>	5.048760	1	2.246945	3.162278	1.938114	1	1.392162	3.162278
	poly(MAP, 2)	66.877958	2	2.859702	1.778279	13.35886	2	1.911800	1.778279
	Grazing	11.600373	1	3.405932	3.162278				
	AMF	6.889240	1	2.624736	3.162278				
	MAT	1.776549	1	1.332872	3.162278				
	<i>Epichloë</i> :poly(MAP, 2)	43.661231	2	2.570538	1.778279	10.96992	2	1.819914	1.778279
	<i>Epichloë</i> :Grazing	10.062159	1	3.172091	3.162278				
	poly(MAP, 2):Grazing	21.600409	2	2.155835	1.778279				
	<i>Epichloë</i> : AMF	5.622520	1	2.371185	3.162278				
	poly(MAP, 2): AMF	2.334877	2	1.236135	1.778279				
	Grazing:AMF	2.678675	1	1.636666	3.162278				
Shoot P (%)		VIF				VIF			
	<i>Epichloë</i>	3.823421				1.152141			
	MAP	6.683975				2.61137			
	Grazing	4.883170				1.551133			
	AMF	5.606159							
	MAT	1.524205							
	<i>Epichloë</i> :MAP	5.403892							
	<i>Epichloë</i> :Grazing	5.786741							
	MAP:Grazing	2.684131				2.306528			
	<i>Epichloë</i> : AMF	4.561121							
	MAP: AMF	1.602869							
	Grazing:AMF	2.429048							
$\Delta^{18}\text{Op}$ (‰)		GVIF	Df	GVIF <sup>1/(2*Df)</sup>	Threshold	GVIF	Df	GVIF <sup>1/(2*Df)</sup>	Threshold
	<i>Epichloë</i>	4.017195	1	2.004294	3.162278				
	poly(MAP, 2)	0.780698	2	2.135084	1.778279	7.904786	2	1.676766	1.778279
	Grazing	6.164886	1	2.482919	3.162278	3.413203	1	1.847485	3.162278
	AMF	5.981332	1	2.445676	3.162278	1.160131	1	1.077094	3.162278

Table S2: cont.

$\Delta^{18}\text{Op}$ (‰)	Initial model				Final model				
		GVIF	Df	$\text{GVIF}^{1/(2*\text{Df})}$	Threshold	GVIF	Df	$\text{GVIF}^{1/(2*\text{Df})}$	Threshold
	Shoot N	7.341899	1	2.709594	3.162278				
	MAT	1.472868	1	1.213618	3.162278				
	<i>Epichloë</i> :poly(MAP, 2)	13.822666	2	1.928182	1.778279				
	<i>Epichloë</i> :Grazing	4.434691	1	2.105871	3.162278				
	poly(MAP, 2):Grazing	18.878645	2	2.084456	1.778279	16.65157	2	2.020058	1.778279
	<i>Epichloë</i> : AMF	5.568388	1	2.359743	3.162278				
	poly(MAP, 2): AMF	1.957660	2	1.182863	1.778279	1.188961	2	1.044220	1.778279
	Grazing:AMF	2.429970	1	1.558836	3.162278				
	<i>Epichloë</i> : Shoot N	7.732291	1	2.780700	3.162278				
	poly(MAP, 2): Shoot N	2.233661	2	1.222515	1.778279				
	Grazing: Shoot N	2.883677	1	1.698139	3.162278				
iWUE		VIF				VIF			
	<i>Epichloë</i>	4.654459							
	MAP	10.349950				2.965429			
	Grazing	8.685052				1.504468			
	AMF	6.903271				1.186036			
	Shoot N	6.434812				1.924508			
	$\Delta^{18}\text{Op}$	8.314657				1.267469			
	MAT	1.651984							
	<i>Epichloë</i> :MAP	7.591687							
	<i>Epichloë</i> :Grazing	9.818894							
	MAP:Grazing	3.150305				2.523829			
	<i>Epichloë</i> : AMF	6.114483							
	MAP: AMF	1.868215				1.091889			
	Grazing:AMF	2.756844							
	<i>Epichloë</i> : Shoot N	6.220056							
	MAP: Shoot N	2.026201							
	Grazing: Shoot N	3.025341				1.921706			
	<i>Epichloë</i> : $\Delta^{18}\text{Op}$	5.706201							
	MAP: $\Delta^{18}\text{Op}$	3.901442							
	Grazing: $\Delta^{18}\text{Op}$	2.444701							

**TABLE S3:** Best-fitting regression models for *Hordeum comosum* analyses. Models included vegetation cover, *H. comosum* cover, *Epichloë* presence, AMF colonization, nitrogen (N) and phosphorus (P) concentration in shoot biomass, and  $\Delta^{18}\text{O}_\text{P}$  and iWUE determined from cellulose extracted from *H. comosum* shoot biomass (see Methods). Columns show the analysis level and characteristics of each model: class, random hierarchies, the family distribution and the link function, variance function, number of observations (n) and parameters (k), and intra class correlation (ICC).

Response variable	Level	Class	Random hierarchies	Family	Link	Variance function	n	k	ICC*
Vegetation cover (%)	Site	gls	no	gaussian	identity	Exp(MAP)	30	4	
<i>H. comosum</i> cover (%)	Site	betareg	no	beta	cauchit		29	4	
<i>Epichloë</i> presence	Plant	glmer	1   Site	binomial	logit		238	3	
AMF colonization (%)	Plant	lme	1   Transect/Site	gaussian	identity	Exp(MAT)	220	7	0.25/0.12
Shoot N (%)	Plant	lme	1   Transect/Site	gaussian	identity	Power(MAT); Exp(MAP)	238	11	0.19/0.19
Shoot P (%)	Plant	lme	1   Transect/Site	gaussian	identity	Exp(MAT)	238	9	0.28/0.23
$\Delta^{18}\text{O}_\text{P}$ (‰)	Plant	lme	1   Site	gaussian	identity	Ident(1  Herbivory)	220	12	0.64
iWUE	Plant	lme	1   Site	gaussian	identity	Power(MAP)	220	12	0.63

\* ICC: Intraclass correlation. The relative values of individual- and group-level variances,  $\sigma^2_\alpha/(\sigma^2_\alpha + \sigma^2_\gamma)$ , which ranges from 0 - if the Site grouping (in this case) conveys no information- to 1 -if all plants in a site are identical.  $\sigma^2_\alpha$  and  $\sigma^2_\gamma$  are random and residual variances, respectively (Gelman & Hill, 2007).

**TABLE S4** Likelihood ratio test of regression models for *Hordeum comosum* analyses. Columns show the models for: vegetation cover, *H. comosum* cover, *Epichloë* presence and AMF colonization, nitrogen (N) and phosphorus (P) concentration,  $\Delta^{18}\text{O}_p$  and iWUE. Rows show the fixed factors, the  $\Delta\text{AIC}$  (AIC null model - AIC best model), the marginal and conditional coefficient of determination ( $R^2_m$  and  $R^2_c$ , respectively). Cells show the probabilities associated with the corresponding LRT statistics. Grey shadow cells indicate factors not included in the corresponding model. Bold numbers indicate significance at p-value < 0.05.

	<i>H. comosum</i> cover (%)	Vegetation cover (%)	<i>Epichloë</i> presence	AMF coloni- zation (%)	Shoot N (%)	Shoot P (%)	$\Delta^{18}\text{O}_p$ (‰)	iWUE
<b>Vegetation cover (%)</b>	0.05							
<b>MAP* (mm)</b>	<b>&lt;0.0001</b>	<b>0.01</b>	<b>0.001</b>	<b>0.0001</b>	<b>0.028</b>	0.87	<b>&lt;0.0001</b>	0.07
<b>MAT (°C)</b>	0.27	0.27	0.93	0.27	0.35	0.87	0.46	0.47
<b>Grazing</b>	0.34	0.12	0.95	0.08	0.58	0.99	0.15	0.30
Grazing x MAP	0.36	0.93	0.15	0.19	0.69	<b>0.0001</b>	<b>0.017</b>	<b>0.02</b>
<b><i>Epichloë</i></b>				<b>0.02</b>	<b>0.01</b>	<b>0.0003</b>	<b>0.35</b>	0.27
<i>Epichloë</i> x Grazing				0.27	0.47	0.96	0.08	0.69
<i>Epichloë</i> x MAP				0.08	<b>0.01</b>	0.50	0.55	0.15
<b>AMF (%)</b>					0.62	0.53	<b>0.03</b>	0.91
<i>Epichloë</i> x AMF					0.69	0.61	0.75	0.15
Grazing x AMF					0.08	0.33	0.96	0.48
MAP x AMF					0.37	0.77	<b>0.046/0.02**</b>	<b>0.06 /0.018**</b>
<b>Shoot N (%)</b>							0.61	0.30
Shoot N x <i>Epichloë</i>							0.24	0.41
Shoot N x Grazing							0.93	<b>0.008</b>
Shoot N x MAP							0.88	0.60
$\Delta^{18}\text{O}_p$ (‰)								<b>&lt;0.0001</b>

**TABLE S4:** cont.

	<i>H. comocum</i> cover (%)	Vegetation cover (%)	<i>Epichloë</i> presence	AMF coloni- zation (%)	Shoot N (%)	Shoot P (%)	$\Delta^{18}\text{O}_p$ (‰)	iWUE
$\Delta^{18}\text{O}_p$ x <i>Epichloë</i>								0.21
$\Delta^{18}\text{O}_p$ x Grazing								0.84
$\Delta^{18}\text{O}_p$ x MAP								0.62
$\Delta\text{AIC}^\dagger$	23.7	11.8	12.35	27.66	15.48	21.42	21.11	19.8
$\text{R}^2_{\text{m}}$	0.32	0.31	0.28	0.32	0.25	0.28	0.50	0.46
$\text{R}^2_{\text{c}}$	-----	-----	0.81	0.57	0.53	0.64	0.82	0.798

\*poly(MAP, 2) in *H. comosum* cover, shoot nitrogen concentration and  $\Delta^{18}\text{O}_p$  models. \*\* Excluding non-important predictor, the p-value decreased from 0.06 to 0.0018.  $\dagger\Delta\text{AIC}$  (AIC null model - AIC best model) where null model is the same model without fixed predictors. As AMF contains NAs, when AMF was not a significant predictor (Shoot nitrogen and phosphorus concentration), we run the model again using the whole dataset (Table S5).

**Table S5:** Likelihood ratio test of regression models for *Hordeum comosum* analyses. Columns show the models for shoot nitrogen and phosphorus concentration. Rows show the fixed factors and the last one the  $\Delta$ AIC (AIC null model - AIC best model). Cells show the probabilities associated with the corresponding LRT statistics. These models excluded AMF as predictor and are justified in the presence of NAs (18) in AMF. As AMF was not important, the model excluding AMF included all observations. Bold numbers indicate significance at p-value < 0.05.

	Shoot N (%)	Shoot P (%)
MAP* (mm)	<b>0.026</b>	0.71
MAT (°C)	0.41	0.82
Grazing	0.77	0.89
<i>Epichloë</i>	<b>0.01</b>	<b>&lt; 0.0001</b>
<i>Epichloë</i> x Grazing	0.79	0.81
<i>Epichloë</i> x MAP	<b>0.008</b>	0.46
Grazing x MAP	0.62	<b>0.0002</b>
$\Delta$ AIC	16.13	26.17

\*poly(MAP, 2) in shoot nitrogen concentration model.

**Table S6:** Post-hoc comparisons of regression models for *Hordeum comosum* analyses. Rows show the models for: shoot nitrogen (N) and phosphorus (P) concentration, iWUE and  $\Delta^{18}\text{O}_\text{P}$ . Columns show the fixed factor, the slope of the numeric factor when suitable, the standard error (SE), the lower and upper limit of the 95% confidence interval (lower.CI and upper.CI, respectively) and the group (where different letters show significant differences between the levels of the corresponding factor with  $p$ -value < 0.05).

<b>Shoot N</b>	<b><i>Epichloë</i></b>	<b>Degree</b>	<b>MAP</b>	<b>SE</b>	<b>lower.CI</b>	<b>upper.CI</b>	<b>Group</b>
	Absent	linear	0.0011225	0.0002907	0.0004674	0.0017775	a
	Present		0.0005073	0.0001615	0.0001433	0.0008713	b
	Absent	quadratic	0.0000039	0.0000012	0.0000012	0.0000066	a
	Present		-0.0000006	0.0000008	-0.0000025	0.0000013	b
<b>Shoot P</b>	<b>Grazing</b>		<b>MAP slope</b>				
	Mild		-0.0001998	5.36e-05	-0.000328	-0.0000715	a
	Severe		0.0001128	4.30e-05	0.000010	0.0002155	b
	<b><i>Epichloë</i></b>		<b>Estimated</b>				
	Absent		0.1596299	0.0168719	0.0895027	0.2297571	a
	Present		0.1958167	0.0153380	0.1320649	0.2595686	b
<b>iWUE</b>	<b>Grazing</b>		<b>MAP slope</b>				
	Mild		0.0206127	0.0057357	0.0070016	0.0342237	a
	Severe		0.0005273	0.0048507	-0.0109836	0.0120383	b
	<b>Grazing</b>		<b>Shoot N slope</b>				
	Mild		-6.592491	2.027127	-11.163172	-2.021810	a
	Severe		2.639470	1.824894	-1.475225	6.754164	b
<b><math>\Delta^{18}\text{O}_\text{P}</math></b>	<b>Grazing</b>		<b>MAP</b>				
	Mild	linear	0.0089617	0.0076958	-0.0083920	0.0263154	a
	Severe		-0.0069360	0.0034044	-0.0146127	0.0007407	a
	Mild	quadratic	-0.0000381	0.0000262	-0.0000968	0.0000206	a
	Severe		0.0000497	0.0000151	0.0000160	0.0000835	b

### 3. APPENDIX S3. SUPPORTING FIGURES

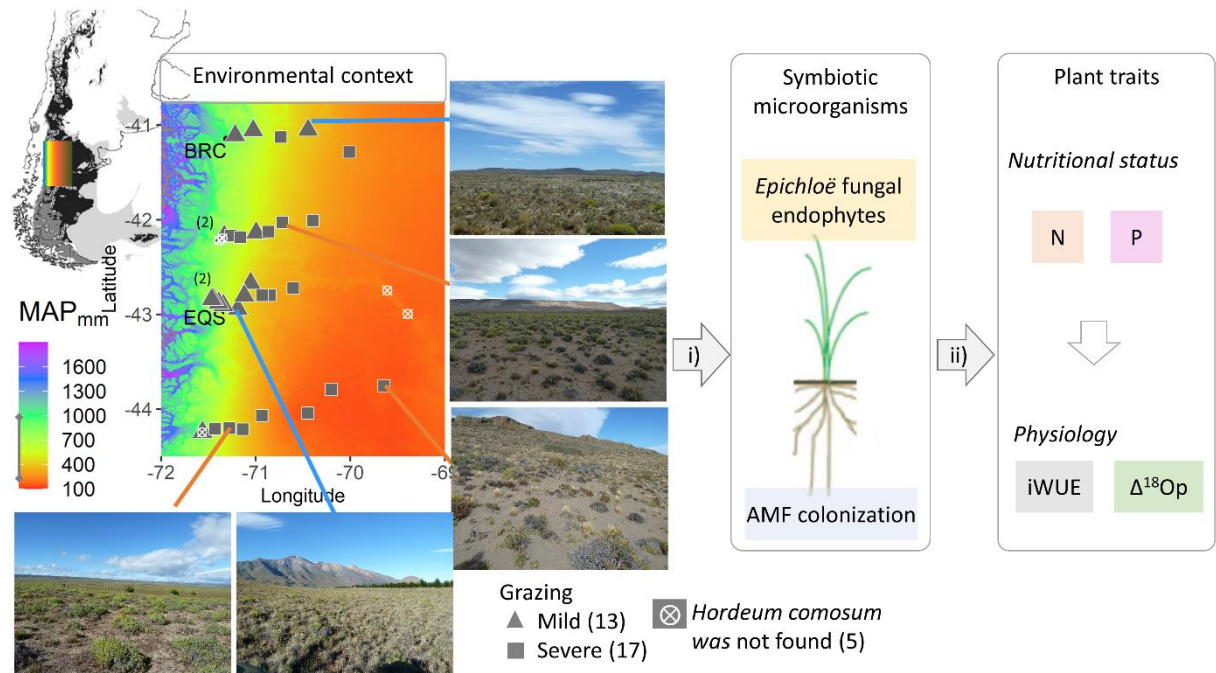


**FIGURE S1** Conceptual analytical framework of the study. We sampled four latitudinally distributed west-east aridity transects in north-west Patagonia, Argentina, considering sites with mild and severe herbivory by domestic and wild grazers, to explore the relationship between the symbiotic status with foliar fungal endophytes (*Epichloë*) and root AMF and eco-physiological traits of the native perennial grass *Hordeum comosum*. Climatic context was mainly determined by mean annual precipitation (MAP) and mean annual temperature (MAT). *H. comosum* plants were not found in three sites in the most humid and two sites in the most arid range of the transects (crossed circle symbol). Analyzed plant traits included N and P concentration, intrinsic water use-efficiency (*i*WUE, the ratio of net photosynthesis and stomatal conductance to water vapor), and  $^{18}\text{O}$ -enrichment of shoot cellulose ( $\Delta^{18}\text{O}_p$ ). Bariloche and Esquel are two main cities indicated as BRC and EQS.

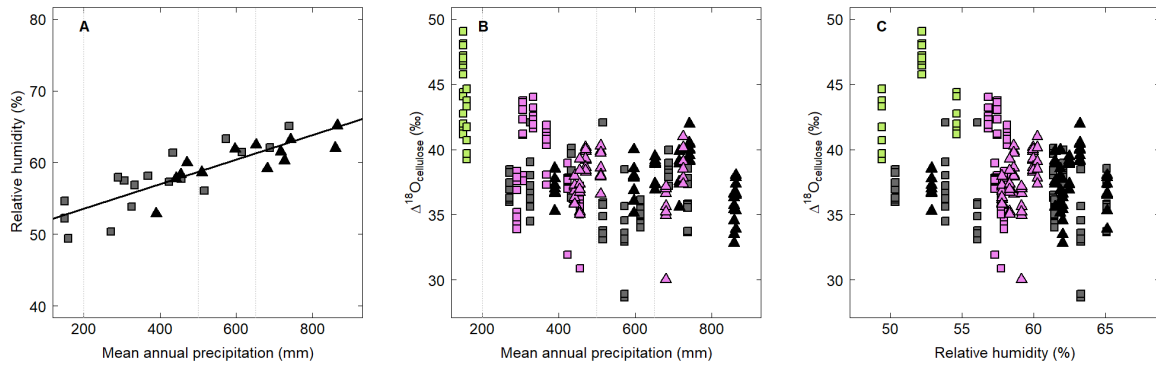


**FIGURE S2** (A) relation between mean annual precipitation (mm, MAP) and relative humidity (% , RH) for the different sites. The full line shows the fit for the linear regression model. Pearson correlation between both variables was 0.84. (B and C)  $^{18}\text{O}$ -enrichment of cellulose ( $\Delta^{18}\text{O}_P = (\delta^{18}\text{O}_P - \delta^{18}\text{O}_{\text{rain}})/(1 + \delta^{18}\text{O}_{\text{rain}})$ ) in shoot biomass of *H. comosum* plants in relation with (B) mean annual precipitation (MAP, mm) and (C) relative humidity (RH, %). Violet dots show  $\Delta^{18}\text{O}_P$  values of *H. comosum* plants growing in sites within the iso-RH of 58.6% (the mean value  $\pm$  2%). Green dots show  $\Delta^{18}\text{O}_P$  values of *H. comosum* plants growing in arid sites (<200 mm MAP). In all cases, symbols indicate *H. comosum* plants from sites with severe (gray squares) and mild (black triangles) level of grazing.

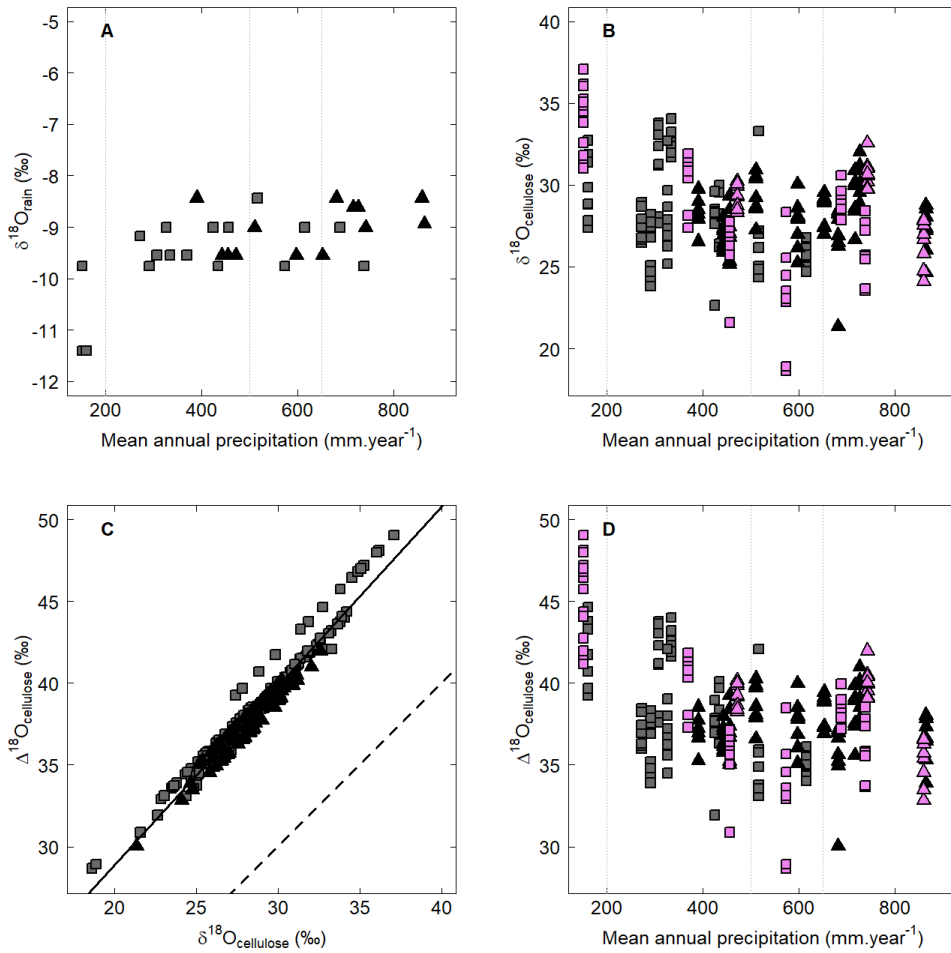


**FIGURE S3** (A) oxygen isotope composition of meteoric waters ( $\delta^{18}\text{O}_{\text{rain}}$ ) in relation to mean annual precipitation (mm). (B) oxygen isotope composition of *H. comosum* shoot cellulose, ( $\delta^{18}\text{O}_{\text{P}}$ ) in relation to mean annual precipitation (MAP, mm). (C)  $^{18}\text{O}$ -enrichment of cellulose ( $\Delta^{18}\text{O}_{\text{P}} = (\delta^{18}\text{O}_{\text{P}} - \delta^{18}\text{O}_{\text{rain}})/(1 + \delta^{18}\text{O}_{\text{rain}})$ ) in relation to  $\delta^{18}\text{O}_{\text{P}}$ . The full line shows the fit for the linear regression model. The dashed line shows the 1:1 relation. (D)  $^{18}\text{O}$ -enrichment of cellulose ( $\Delta^{18}\text{O}_{\text{P}}$ ) in relation to mean annual precipitation (MAP, mm). Violet dots in (B) and (D) denote plants growing in sites within an isothermal of  $8.4^{\circ}\text{C}$  ( $\pm 0.25^{\circ}\text{C}$ , i.e., from mean MAT plus  $0.5^{\circ}\text{C}$  (from  $8.15$  to  $8.65^{\circ}\text{C}$ ). In (A, B and D) vertical dotted lines delimit aridity zones by MAP range: humid ( $>650$  mm), dry subhumid ( $650$  to  $500$  mm), semiarid ( $500$  to  $200$  mm), and arid ( $<200$  mm). Note the small site-by-site variation of  $\delta^{18}\text{O}_{\text{rain}}$  (A) in comparison with the variation

of  $\Delta^{18}\text{O}_\text{P}$  (B). In all cases, symbols indicate *H. comosum* plants from sites with severe (gray squares) and mild (black triangles) level of grazing.

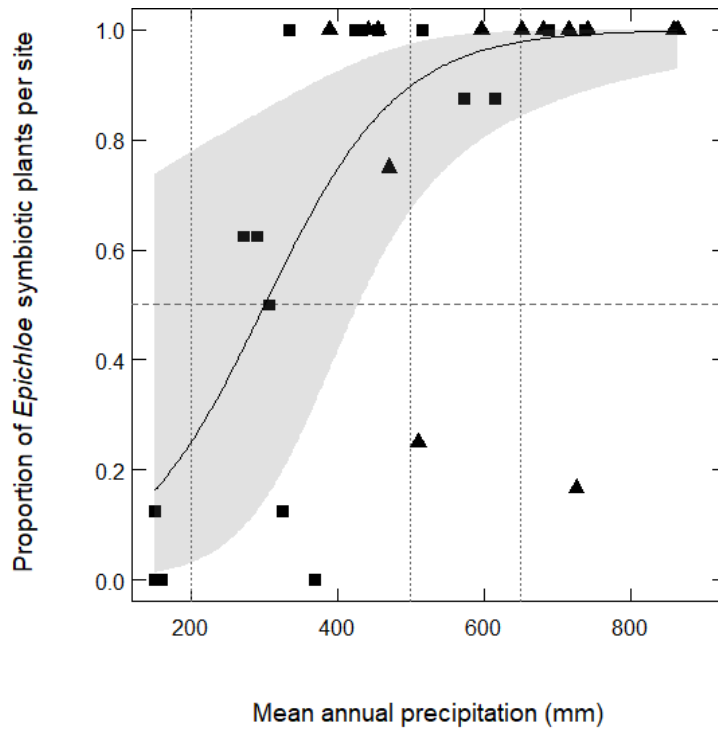


**FIGURE S4** Proportion of *Epichloë* symbiotic plants per site in relation to mean annual precipitation (MAP, mm). Symbols show *H. comosum* plants from sites with severe (squares) and mild (triangles) levels of grazing. Full line and shadow show model fit and 95% prediction interval, respectively. Vertical dotted lines delimit the environments determined by MAP range: humid (>650 mm), dry subhumid (650 to 500 mm), semiarid (500 to 200 mm), and arid (<200 mm).

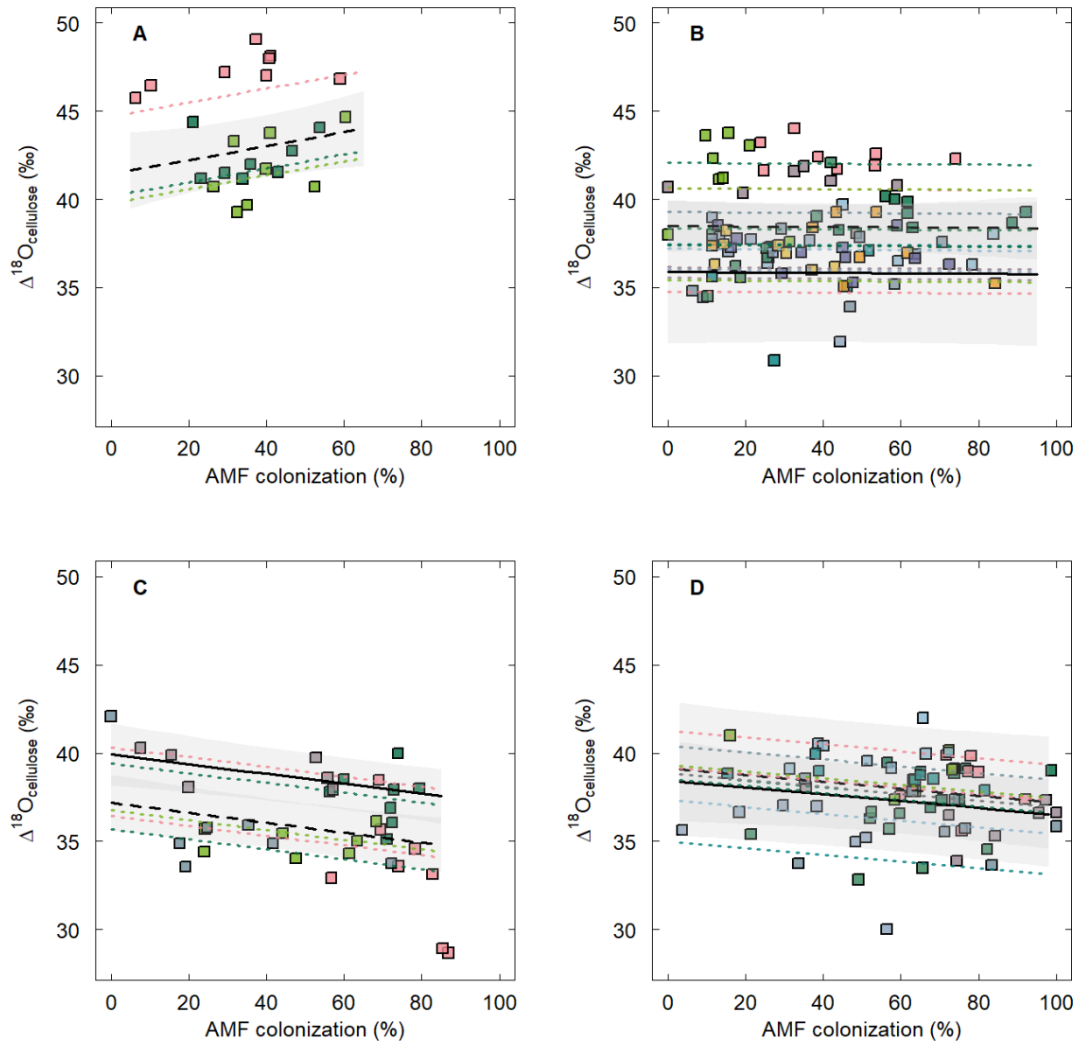


**FIGURE S5**  $^{18}\text{O}$ -enrichment of cellulose ( $\Delta^{18}\text{O}_{\text{P}}$ ) in shoot biomass of *H. comosum* plants in relation with the degree of arbuscular mycorrhizal colonization (AMF, %). Each panel shows an environment corresponding to (A) arid (MAP <200 mm), (B) semiarid (MAP 200 – 500 mm), (C) subhumid (MAP 500 – 650 mm) and (D) humid (MAP > 650 mm). Symbols show individual plants. Different sites are distinguished by color. Full and dashed black lines show the fit for mild and severe grazing conditions, respectively, according to the regression model presented in Table 1 and Table S2-S6 for the MAP and AMF values according to the corresponding environment. Shadows show 95% prediction intervals. Dash colored lines show the fit for the corresponding site (i.e., random effect).

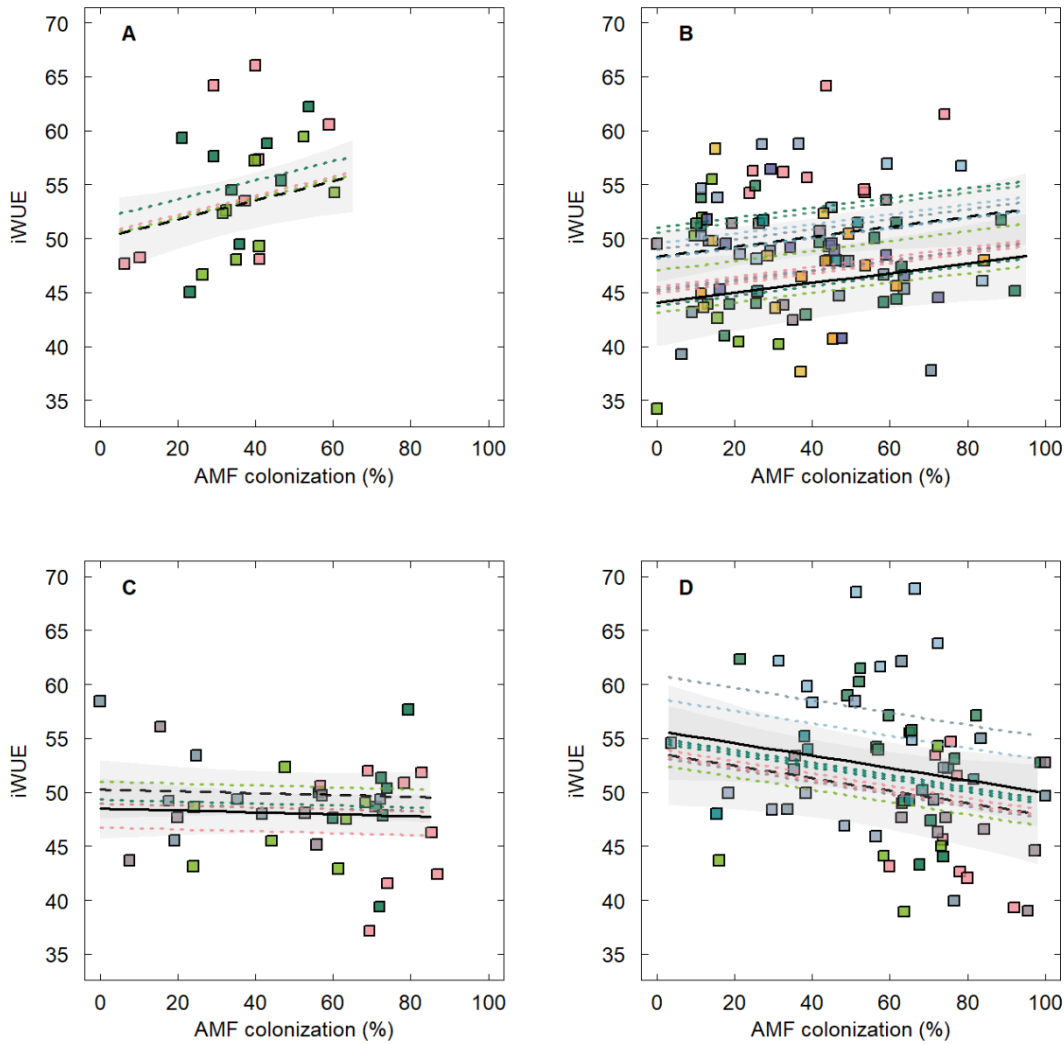


**FIGURE S6** iWUE of cellulose in shoot biomass of *H. comosum* plants in relation with the degree of arbuscular mycorrhizal colonization (AMF, %). Panels: (A) arid (MAP < 200 mm), (B) semiarid (MAP 200 – 500 mm), (C) subhumid (MAP 500 – 650 mm) and (D) humid (MAP > 650 mm) environments. Symbols show individual plants. Different sites are distinguished by color. Full and dashed black lines show the fit for mild and severe grazing conditions, respectively, according to the regression model presented in Table 1 and Table S2-S6 for the MAP and AMF values according to the corresponding environment. Shadows show 95% prediction intervals. Dash colored lines show the fit for the corresponding site (i.e., random effect).

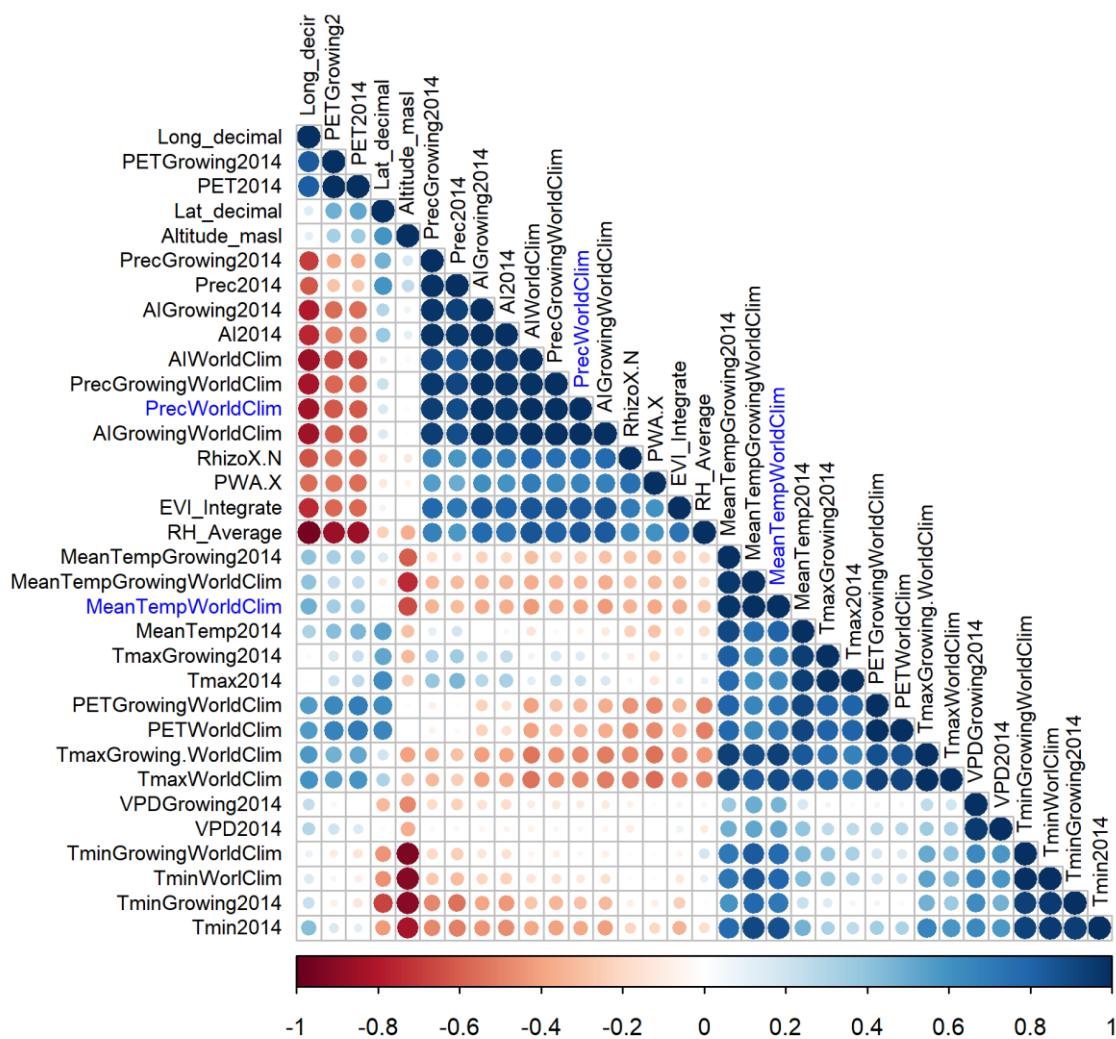


**FIGURE S7** Pearson correlation between climatic, geographical coordinates, elevation, the enhanced vegetation index (EVI) and soil [N concentration in the rhizosphere (RhizoX.N) and potential soil water availability (PWA.X)] variables. The climatic variables precipitation (Prec), potential evapotranspiration (PET) and temperatures (Tmin, Tmax and MeanTemp) were calculated for the annual average and for the growing season of *H. comosum* [WorldClim and GrowingWorldClim, respectively; obtained from 50-year climatic means (1950-2000) of the WorldClim database]. The same climatic variables were estimated for the sampling-year and sampling-year growing season (2014 and Growing2014, respectively). The size of the circle and the color intensity indicate the value of the correlation following the reference below. Filled cells indicate highly correlated variables.

Variables used in the corresponding statistical models were mean annual precipitation (PrecWorldClim) and mean annual temperature (MeanTempWorldClim; both in blue labels). See Method S1 for details about the variables.

## 4. REFERENCES

- Allen, R. G., Pereira, L. S., Raes, D., & Smith, M. (1998). Crop evapotranspiration - Guidelines for computing crop water requirements. In *Irrigation and Drainage Paper No. 56*, FAO (p. 300). FAO. <https://doi.org/10.1016/j.eja.2010.12.001>
- Baca Cabrera, J. C., Hirl, R. T., Schäufele, R., Macdonald, A., & Schnyder, H. (2021). Stomatal conductance limited the CO<sub>2</sub> response of grassland in the last century. *BMC Biology*, *19*(50), 50. <https://doi.org/https://doi.org/10.1186/s12915-021-00988-4>
- Barbour, M. M. (2007). Stable oxygen isotope composition of plant tissue: a review. *Functional Plant Biology*, *34*(2), 83–94. <https://doi.org/10.1071/FP06228>
- Barton, K. (2016). *MuMIn: Multi-Model Inference*. R package version 1.15.6. <https://cran.r-project.org/package=MuMIn>
- Bates, D., Maechler, M., Bolker, B., & Walker, S. (2015). *lme4: Linear mixed-effects models using eigen and S4*. R package version 1.1–7. 2014. <https://doi.org/10.1016/j.jorganchem.2015.04.040>
- Bonvissuto, G. L., Somlo, R. C., Lanciotti, M. L., González Carteau, A., & Busso, C. (2008). *Guías de condición para pastizales naturales de “Precordillera”, “Sierras y Mesetas” y “Monte Austral” de Patagonia*. INTA EEA Bariloche–Global Environment Facility: Patagonia.
- Cernusak, L., Farquhar, G., & Pate, J. (2005). Environmental and physiological controls over oxygen and carbon isotope composition of Tasmanian blue gum, *Eucalyptus globulus*. *Tree Physiology*, *25*(2), 129–146. <https://doi.org/https://doi.org/10.1093/treephys/25.2.129>
- Defossé, G. E., Bertiller, M. B., & Ares, J. O. (1990). Above-ground phytomass dynamics in a grassland steppe of Patagonia, Argentina. *Journal of Range Management*, *43*(2), 157–160. <https://doi.org/10.2307/3899036>
- Dormann, C. F., Elith, J., Bacher, S., Buchmann, C., Carl, G., Carré, G., Marquéz, J. R. G., Gruber, B., Lafourcade, B., Leitão, P. J., Münkemüller, T., McClean, C., Osborne, P. E., Reineking, B., Schröder, B., Skidmore, A. K., Zurell, D., & Lautenbach, S. (2013). Collinearity: A review of methods to deal with it and a simulation study evaluating their performance. *Ecography*, *36*(1), 027–046. <https://doi.org/10.1111/j.1600-0587.2012.07348.x>
- Farquhar, G. D., Cernusak, L. A., & Barnes, B. (2007). Heavy water fractionation during transpiration. *Plant Physiology*, *143*(1), 11–18. <https://doi.org/10.1104/pp.106.093278>
- Fuka, D., Walter, M., Archibald, J., Steenhuis, T., & Easton, Z. (2014). *EcoHydRology: A community modeling foundation for Eco-Hydrology*. R package version 0.4.12. <https://cran.r-project.org/package=EcoHydRology>
- Gelman, A., & Hill, J. (2007). *Data Analysis Using Regression and Multilevel/Hierarchical Models* (R. M. Alvarez, N. L. Beck, & L. L. Wu (eds.)). Cambridge Univ Press.
- Hijmans, R. J., Cameron, S. E., Parra, J. L., Jones, P. G., & Jarvis, A. (2005). Very high resolution interpolated climate surfaces for global land areas. *International Journal of Climatology*, *25*(15), 1965–1978. <https://doi.org/10.1002/joc.1276>
- Hirl, R. T., Ogée, J., Ostler, U., Schäufele, R., Baca Cabrera, J. C., Zhu, J., Schleip, I., Wingate, L., & Schnyder, H. (2021). Temperature-sensitive biochemical <sup>18</sup>O-fractionation and humidity-dependent attenuation factor are needed to predict δ<sup>18</sup>O of cellulose from leaf water in a grassland ecosystem. *New Phytologist*, *229*(6), 3156–3171. <https://doi.org/10.1111/nph.17111>
- Kahmen, A., Sachse, D., Arndt, S. K., Tu, K. P., Farrington, H., Vitousek, P. M., Dawson, T. E., Designed, T. E. D., & Performed, H. F. (2011). Cellulose δ<sup>18</sup>O is an index of leaf-to-air vapor pressure difference (VPD) in tropical plants. *Proceedings of the National Academy of Sciences of the United States of America*, *108*(5), 1981–1986. <https://doi.org/10.1073/pnas.1018906108>
- Lenth, R. V. (2017). *emmeans: Estimated Marginal Means, aka Least-Squares Means*. R package version 1.0. <https://cran.r-project.org/package=emmeans>
- Ma, W. T., Tcherkez, G., Wang, X. M., Schäufele, R., Schnyder, H., Yang, Y., & Gong, X. Y. (2021). Accounting for mesophyll conductance substantially improves <sup>13</sup>C-based estimates of intrinsic water-use efficiency. *New Phytologist*, *229*(3), 1326–1338. <https://doi.org/10.1111/nph.16958>
- McGonigle, T. P., Miller, M. H., Evans, D. G., Fairchild, G. L., & Swan, J. A. (1990). A new method

- which gives an objective measure of colonization of roots by vesicular-arbuscular mycorrhizal fungi. *New Phytologist*, 115(3), 495–501. <https://doi.org/10.1111/j.1469-8137.1990.tb00476.x>
- Nakagawa, S., & Freckleton, R. P. (2008). Missing inaction: the dangers of ignoring missing data. *Trends in Ecology and Evolution*, 23(11), 592–596. <https://doi.org/10.1016/j.tree.2008.06.014>
- Nakagawa, S., & Freckleton, R. P. (2011). Model averaging, missing data and multiple imputation: A case study for behavioural ecology. *Behavioral Ecology and Sociobiology*, 65(1), 103–116. <https://doi.org/10.1007/s00265-010-1044-7>
- Pinheiro, J., & Bates, D. (2006). *Mixed-Effects Models in S and S-PLUS* (J. Chambers, W. Eddy, W. Härdle, S. Sheather, & L. Tierney (eds.)). Springer.
- R Development Core Team. (2019). *R: a language and environment for statistical computing* (3.6.1; p. Vienna, Austria). R Foundation for Statistical Computing. <https://www.r-project.org/>.
- RStudio, T. (2019). *RStudio: Integrated Development for R* (1.2.1335). RStudio, Inc. <http://www.rstudio.com/>.
- Saxton, K., & Rawls, W. (2006). Soil water characteristic estimates by texture and organic matter for hydrologic solutions. *Soil Science Society of America Journal*, 70, 1569–1578. <https://doi.org/10.2136/sssaj2005.0117>
- Scheidegger, Y., Saurer, M., Bahn, M., & Siegwolf, R. (2000). Linking stable oxygen and carbon isotopes with stomatal conductance and photosynthetic capacity: a conceptual model. *Oecologia*, 125(3), 350–357. <https://doi.org/10.1007/s004420000466>
- Schielzeth, H. (2010). Simple means to improve the interpretability of regression coefficients. *Methods in Ecology and Evolution*, 1(2), 103–113. <https://doi.org/10.1111/j.2041-210x.2010.00012.x>
- Siffredi, G. L., Boggio, F., Giorgetti, H., Ayesa, J. A., Kropfl, A., & Alvarez, J. M. (2011). *Guía para la Evaluación de Pastizales para las Áreas Ecológicas de Sierras y Mesetas Occidentales y de Monte de Patagonia Norte*. Ediciones Instituto Nacional de Tecnología Agropecuaria.
- UNEP. (1992). *World atlas of desertification* (E. Arnold (ed.)).
- van Reeuwijk, L. P. (2002). *Procedures for Soil Analysis* (6th ed.). International Soil and Reference Information Centre. Food and Agriculture Organisation.
- Werner, M. (2019). *ECHAM5-wiso simulation data - present-day, mid-Holocene, and Last Glacial Maximum*. PANGAEA. <https://doi.org/10.1594/PANGAEA.902347>
- Wittmer, M., Auerswald, K., Tungalag, R., Bai, Y. F., Schäufele, R., Bai, C. H., & Schnyder, H. (2008). Carbon isotope discrimination of C3 vegetation in Central Asian Grassland as related to long-term and short-term precipitation patterns. *Biogeosciences Discussions*, 5(1), 903–935. <https://doi.org/10.5194/bgd-5-903-2008>
- Zuur, A. F., Ieno, E. N., Walker, N. J., Saveliev, A. A., & Smith, G. M. (2009). *Mixed Effects Models and Extensions in Ecology with R* (M. Gail, K. Krickeberg, J. M. Samet, A. Tsiatis, & W. Wong (eds.)). Springer.